Renewable and Sustainable Energy Reviews 25 (2013) 831–843

Contents lists available at SciVerse ScienceDirect

Renewable and Sustainable Energy Reviews

journal homepage: www.elsevier.com/locate/rser

Distributed solar electricity generation across large geographic areas, Part I: A method to optimize site selection, generation and storage

Wolf D. Grossmann [a,b], Iris Grossmann [c,*], Karl W. Steininger [a,d]

[a] Wegener Center for Climate and Global Change, University of Graz, Leechgasse 25, A-8010 Graz, Austria
[b] International Center for Climate and Society, University of Hawaii at Manoa, 1680 East–West Road, Honolulu, HI 96822, USA
[c] Center for Climate and Energy Decision Making, Carnegie Mellon University, 5000 Forbes Ave, Pittsburgh, PA 15213, USA
[d] Department of Economics, University of Graz, Universitaetsstr. 15, A-8010 Graz, Austria

ARTICLE INFO

Available online 15 October 2012

Keywords:
Large-scale solar energy network
Renewable energy storage
Photovoltaics and concentrating solar power
Intermittency
Desertec
High voltage direct current

ABSTRACT

Perhaps the greatest obstacle to large-scale solar energy generation is the intermittent nature of solar energy and the associated costly storage. This paper presents a method to optimize combinations of selected worldwide regions in different time zones with the surprising capability of providing sufficient electricity generation to overcome intermittency or reduce it to such an extent that substantially less storage and generation capacity are needed. The recent sharp drop in the cost of photovoltaic (PV) generation capability accompanied by worldwide increased investment in PV plants suggests a new economic base for cooperative efforts to sequentially combine day time insolation. The approach presented here optimizes two aspects, first, the selection of sites across large geographic areas, and second, the size and relative proportion of generation and storage capacity at each site. Our approach converts 20 years of daily insolation data by NASA Solar Sizer to hourly scale. The hourly data are used to assess and compare supranational distributed solar networks in different parts of the globe that have recently been proposed, and to subsequently optimize their generation capacity and storage. We show that linking regions in different time zones and on the two hemispheres can fully eliminate intermittency without the need for fuel and renewable energy other than solar.

Contents

1. Introduction

Photovoltaic (PV) generation of electricity has become competitive in a large number of regions and costs are projected to

* Corresponding author. Tel.: +1 412 268 5489; fax: +1 412 268 3757.
E-mail address: irisg@andrew.cmu.edu (I. Grossmann).

1364-0321/$ - see front matter © 2012 Elsevier Ltd. All rights reserved.
http://dx.doi.org/10.1016/j.rser.2012.08.018

decline further [1]. Manufacturing costs of PV modules have decreased by 60% between 2008 and the end of 2010 to \$0.7/Wp [2–4], resulting in grid parity in parts of California, Hawaii and Spain [2,3,5]. The breakthrough in competitiveness became widely visible in new contracts signed in 2012 for three PV plants of considerable size (350 MW, 400 MW and 500 MW) in Extremadura, Spain [6,7]. The 400 MW installation will cost \$571 m; yet the plants will not be subsidized, signaling a new stage in PV electricity generation.

In the last few years, the rapid decrease of costs, technological advances [8–12] and policy support for renewable energy have encouraged large investments into solar energy generation capacity [4]. In early 2010 more than 100 countries had enacted renewable energy policies, up from 55 countries in 2005 [4], with global investments of \$211 billion in 2010, a 540% rise since 2004 [13]. Also in 2010, developing economies overtook developed ones in terms of new financial investments into renewable energy [13]. PV capacity has grown at the highest rate of all renewables. In 2010, installed PV capacity grew at rates exceeding 70%, compared to wind at a rate of 25%, and reached a total installed capacity of 40 GW, while concentrated solar power (CSP) reached 1.1 GW [4].

Can solar energy become significant? The technical potential of solar energy has been estimated at above 420 TW, while the total potential of the other common renewables is estimated between 4.4 TW and 75.6 TW [14,15]. Significant extensions to the share of electricity in energy supply are thinkable; e.g., if most vehicles became electric, solar could supply another 4 TW or 25% of the current global energy consumption. All indicators for judging energy sources are very favorable for PV, including its low specific demand for area, good availability of resources, longevity, low costs of operation and maintenance, reliability and low environmental impacts with an energy payback time of less than one year [15].

However, a present total installed capacity of 41.1 GW is low in comparison with the global energy consumption of 17 TW in 2010 [16]. This is even more so as solar has a capacity factor of only up to 27%, giving an effective generation capacity for those 41.1 GW of $41.1 \times 0.27 = 11.1$ GW. Installed PV has grown by a factor of 22 between 2001 and 2010, which is one doubling every two years. If PV continued growing at this rate, it could supply the 2.1 TW of global electricity demand within 15 years, which implies a decrease of global primary energy use by $\sim$6.8 TW, and it could supply 17 TW within 21 years. The almost general expectation is that the growth rate will level off because it depends on subsidies and portfolios. However, although in 2011 most countries had decreased their subsidies, the global installed PV capacity has doubled in that year. First Solar, the price leader in thin-film PV panels, expects that sales of PV will no longer need subsidies after 2014. In the past First Solar has consistently outperformed its own projections. A remaining major hurdle, however, is the intermittent nature of solar electricity.

Intermittency is due to the variation of solar irradiance with the cycle of day and night, the weaker irradiance and shorter days during winter, and attenuation due to clouds, dust, and volcanic activity. Here we show that linking regions in different time zones and on the two hemispheres can significantly reduce or fully eliminate intermittency so that neither fuel nor renewable energy other than solar are needed. The method presented allows us in particular to review previously proposed large-scale schemes of solar energy generation and to determine improved schemes.

We optimize two aspects, first, the selection of sites across large geographic areas, and second, the size and relative proportion of generation and storage capacity for the selected sites. We first choose 67 sites throughout the world as candidate sites; additional sites can be added or the model can be limited to a world region of interest. Our model then compares combinations of sites drawn from this set to determine a combination that allows meeting a given load with minimal generation capacity and storage. The user can specify whether to minimize generation capacity for a given amount of storage, minimize storage for given generation capacity or minimize the generation cost of electricity. Each option gives feasible pairs of generation capacity and storage. Different combinations of locations are here referred to as "configurations". The optimization procedure uses 20 years of daily solar insolation data (1986–2005) from NASA Solar Sizer [17] which is available for the whole world. After scaling these daily values to hourly values, the model determines the available insolation from different combinations of sites given the time zone and insolation pattern of each site. It then determines the required storage and generation capacity to meet the load throughout the varying weather conditions during 1986–2005. The usage of 20 years of insolation data is important to ensure that storage and generation are sufficient for a variety of weather conditions, including prolonged periods with little or no insolation. We apply this method to review several recently proposed supranational schemes of distributed solar energy generation and identify improved configurations.

In Section 2 we review the development of solar energy costs. In Section 3 we describe the hourly scaling method and present a sensitivity analysis. In Section 4 we review recently proposed large-scale schemes of solar generation and identify improved configurations that need substantially less storage and/or generation capacity. The schemes discussed include the EUMENA scheme that links electricity generation in the Sahara and Europe [18–23], the "Solar Grand Plan" proposed by Zweibel et al. [24] that would supply 69% of the US electricity needs from solar, wind and geothermal by 2050, and the GRENATEC plan that would link Australia and Asia [25–27]. While these plans rely on solar energy generation on a much larger scale than previously considered, both the EUMENA network and the Solar Grand Plan require considerable excess generation capacity and large storage capacity to address intermittency. We show that for all three schemes, the problems of intermittency and excess capacity and storage can be substantially improved through optimal site combinations. For an easier comparison of schemes we assume constant demand throughout the year; but we also show how our approach can meet nonlinear demand curves such as the actual demand of 27 European countries during 2011. We also discuss a China–Mongolia configuration, given the current rapid development of solar energy generation in China and Mongolia [26,28,29].

2. Background: Recent cost development of solar electricity

The concept of grid parity compares the cost of solar electricity with the costs of electricity from the grid. Solar achieves grid parity when its costs per kWh are the same as costs from the grid. Grid parity is a relative concept; it depends on the absolute costs of both, electricity generated by conventional sources and from solar. For example, electricity costs are high in Italy but low in France. PV has reached grid parity in parts of Italy between 2010 and 2011 [30], but grid parity in France will take longer [1].

The levelized cost of electricity (LCOE) includes capital costs, depreciation, operation, maintenance, management etc. LCOE allows a direct comparison of the costs of all types of electricity generation. LCOE of all forms of renewable energy has decreased considerably in the last five years. We calculate LCOE of 8.4 ¢/kWh for a 400 MW PV plant at costs of \$571 m, taking into account the insolation in Extremadura/Spain of 1729 kWh/m^2/year (20-year average of solar data for Extremadura from NASA [17]) and with LCOE calculated according to Zweibel 2005 [31]. For comparison, BNEF [1] gives LCOE in Q1 2012 starting at \$0.11/kWh.

The systems price for a complete installation of PV consists of costs for the PV module plus the balance of system (BOS). BOS denotes electronics, parts and labor for panel installation and grid connection. In addition to the decrease in manufacturing costs of PV modules by 60% between 2008 and the end of 2010 [1,3,4] to \$0.7/Wp, the sales price of PV have decreased by another 60% thereafter in just one year, 2011 [32]. This last decrease was faster than the decrease of manufacturing costs [32,33]. Most manufacturers of PV modules are now in the red, several went bankrupt. The stock price of First Solar, a leading manufacturer, fell within one year from \$120 to \$14 (May 2012). These present sales prices are not sustainable without substantive further decrease of manufacturing costs, which are expected given economies of scale in manufacturing, strong competition and significant decrease also in the costs of the BOS [15,1]. Recently costs of panel manufacturing decreased to \$0.65/Wp whereas costs of BOS decreased to \$0.87/Wp [34]. This gives a systems price of \$1.67/Wp at the 2012 gross margin of 10%, which correspond to costs of 7.35 ¢/kWh (based on [31] for Californian desert areas with 2300 kWh/m^2/year). In 2010 the margin for First Solar was still at 50%, i.e., electricity costs >11 ¢/kWh.

Some experts indicate low costs of 20 ¢/Wp each for both PV and BOS [35], which together with a margin of e.g., 15–20% corresponds to electricity costs of 2.1 ¢/Wp in desert areas. Solarbuzz predicts wafer prices of \$0.25/Wp for 2013 [36] (but assembling wafers into panels increases costs). First Solar, which has made very conservative projections so far, sees systems manufacturing costs of below \$1.20/Wp including 15% to 20% margin in 2016. These costs give LCOE of 5.2 ¢/kWh in desert regions with an annual insolation of 2300 kWh/m^2, following the calculation in [31]. Fthenakis et al. [37] calculate average costs of 2 ¢/kWh for transportation of this electricity from the desert regions in the US Southwest to consumers in the US giving a price of 7.6 ¢/kWh including a margin of 20% on transmission in the electricity grid. Average retail price of electricity in 2011 in the US was between 6.2 ¢/kWh and 25.1 ¢/kWh; average price was 10.1 ¢/kWh [38]. Whereas some of the low costs mentioned above are rather extreme, PV does no longer need a dramatic decrease of costs to become a major factor. If the historic decrease of manufacturing costs for PV systems would now level of in an S-shaped curve, solar electricity generation might become the cheapest form of electricity generation. But it has one remaining problem, its intermittency.

3. Methods

The intermittent character of solar irradiance is due to several factors, the cycles of day and night, weaker irradiance and shorter days during winter, and attenuation from clouds, dust or even volcanic activity. Recent work has targeted the optimization of individual solar generation and storage systems [40,41], but not the optimization of distributed solar networks covering very large geographic areas and multiple time zones. To systematically explore the elimination of intermittency through linking generation sites in different time zones we use daily insolation data by NASA Solar Sizer [17]. The global availability of these data on a $1^\circ \times 1^\circ$ grid with the same temporal and spatial resolution and same definition across geographic regions makes our method globally applicable.

In contrast to other approaches e.g., [42], our method does not require data on cloudiness. To ensure robustness with respect to infrequent situations of very low insolation (such as longer cloudy periods or periods of simultaneous cloudiness at different sites), configurations of solar generation sites have to be evaluated over decades using historical insolation data. Moreover both temporal and spatial resolution have to be sufficiently fine. Consequently we use daily data for the 20 years 1986–2005 (no later data are available) which we convert to hourly scale. Attention is paid to the five leap days. To ensure robustness with respect to the scaling method, we additionally derive a lower and upper boundary for the required storage.

3.1. Methods for translating daily insolation data into hourly data

Each configuration is treated as a system consisting of generation capacity, storage, load, and management of storage. For configurations with at least two time zones, hourly data are necessary. In general, hourly data are available only for some regions, and data for different regions usually differ in definition and spatial resolution. Solar Sizer data is available globally and is consistent across regions, but it is on a daily scale. We will proceed in several steps to derive hourly scaled data and discuss the sensitivity of each step.

In a straightforward calculation without consideration of time zones (referred to as Method 1 or M1), the insolation from all sites in a given configuration is added up for each day. The sum of insolation times the capacity of the PV cells gives the generated electricity. For M1, electricity is added to the system at 0:00 UTC (Universal Coordinated Time, i.e., Greenwich Time), and the load is subtracted hourly. The remaining electricity is added to the storage as long as capacity allows. If the daily load is higher than the electricity generated, the deficit is covered from storage while possible. If the storage does not suffice, either generation capacity or storage or both must be increased.

The next method, M2, uses time zones. We add the insolation of each site into the system at sunset of that site rather than in advance at 0:00 UTC. Here, the storage has to fill the assumed gap between two sunsets, resulting in unrealistically high storage. The next method, M3, has to account for the fact that solar irradiation is not concentrated within one hour but is distributed over the day. M3 considers the theoretically possible maximum irradiation for a given site, the clear sky value. However, the temporal pattern of irradiation in desert areas is mostly similar to the pattern of the clear sky value. The daily pattern of the clear sky value is proportional to the cosine of the declination of the sun over a given site during a given day [43]. We distribute daily insolation proportional to this form by multiplying the clear sky value for a specific time with the ratio of insolation for that day divided by the integral over the clear sky value of that day. The form of the clear sky value is calculated with standard trigonometric functions [43] and the Fourier series representation for the declination (the height of the sun over the equator relative to the axial tilt of the earth) given by Spencer [44]. Many different approaches exist to calculate the clear sky value. For preservation of consistency in definitions, we calibrate the form of the clear sky value with the maximum insolation value from Solar Sizer over the time series of 20 years. This approximation to the actual distribution of solar radiation begins at sunrise, has its peak at noon and ends at sunset of that location. The clear sky value is a theoretical upper limit because even in desert areas actual irradiation is below the clear sky value most of the time. M3, which follows this pattern, gives the longest time span for which irradiation can arrive at a given site, and hence provides a lower boundary for storage.

M3 also has shortcomings; the pattern of solar irradiation can be different if insolation for a given day is below the theoretical maximum. For example, if the daily insolation is at 50% of its possible maximum, all irradiation could arrive during the first or second half of the day. To derive an upper boundary for the required storage, we consider the case when the full amount of insolation for a day arrives as close as possible to sunset.

This requires that consumption during that day is met from storage before any new insolation has arrived. Thus, the storage has to be large enough to provide electricity prior to the arrival of insolation and it has to have enough stored electricity from the previous day. The worst case for the storage of a given configuration occurs when insolation is minimal on a given day followed by a second day on which insolation at all sites arrives as late as possible. Hence an upper boundary for the storage needed by the configuration can be calculated by identifying the minimum daily total insolation during the 20 years considered and applying M2, which assumes that all electricity is added at sunset. This upper boundary could be improved, i.e., lowered, by assuming that irradiation arrives close to sunset but is distributed according to the shape of the clear sky value.

Fig. 1 compares the different methods. Fig. 1 shows that M3 gives the best approximation to the actual distribution of irradiation for days without or with low attenuation. The daily sum of the hourly values resulting from M3 equals the daily insolation value (as one would expect). Likewise the sum of the area below the curve given by each of the other methods equals the daily insolation. Fig. 2 shows the distribution of irradiation for sites in Eastern and Western Australia, the Saudi desert, the Western Sahara, the Atacama desert and the Mojave desert according to M3 (note the different dimension and scaling of the vertical axis compared to Fig. 1). This is the pattern of insolation received by desert areas on most days when insolation is close to its maximum. The figure also shows that there is considerable overlap of irradiation in these six sites during northern winter (December 21).

The calculation of necessary storage is sensitive to the method used to approximate irradiation, whereas the calculation of generation capacity is far less sensitive. This is because the amount of insolation is the same for all methods and the resulting electricity is directly proportional to the generation capacity and insolation. Hence, if the same generation capacity is used for all methods, the same amount of electricity is generated, only the timing of generation differs. Balancing gaps in irradiation is the task of storage. Consequently, the results for necessary storage differ between methods. Actual storage demand is between the numbers given by M3 (where irradiation is spread perfectly across the day according to the clear sky value, thus giving the lower bound for storage) and M2 where insulation is assumed to arrive at sunset, thus giving an upper boundary. This is exactly what is needed for our purposes. With these upper and lower limits, a review of previously proposed networks is facilitated. In comparison, more rapid changes of irradiation do not severely tax the storage because shortcomings in irradiation are much shorter. This is a crucial observation as it means that our method is not sensitive to rapid fluctuations in insolation during the day.

Fig. 3 (top panel) compares measured hourly insolation in the Mojave [45] with the values obtained with M1, M2, and M3. Measured hourly data are available only for select locations. The bottom panel compares measured hourly insolation with hourly values from M3; here we have selected a period of time with noticeable differences between the measured and the calculated values. However, as we will discuss in the following, the calculated values are better than they look in Fig. 3. Solar irradiation from M3 starts and ends at the same time as the measured data. The other methods have no coincidence with the real pattern; only the amount of insolation is the same for all methods. For most days the measured hourly irradiation in this figure is greater than the irradiation according to M3, although M3 follows the clear sky value and the integral over the irradiation from M3 for

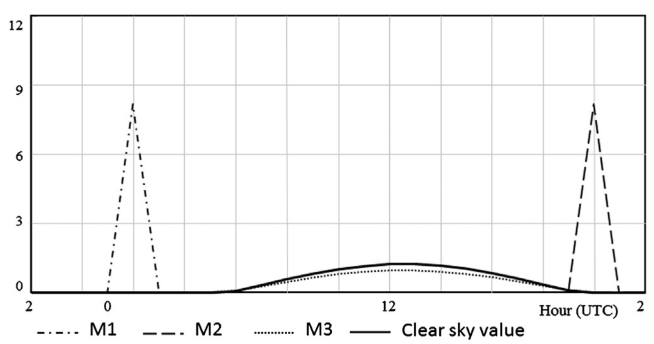


Fig. 1. The three methods to approximate daily solar insolation (with M3 and M2 providing, respectively, a lower and upper boundary for insolation) for the Atacama Desert, December 21, 1986.

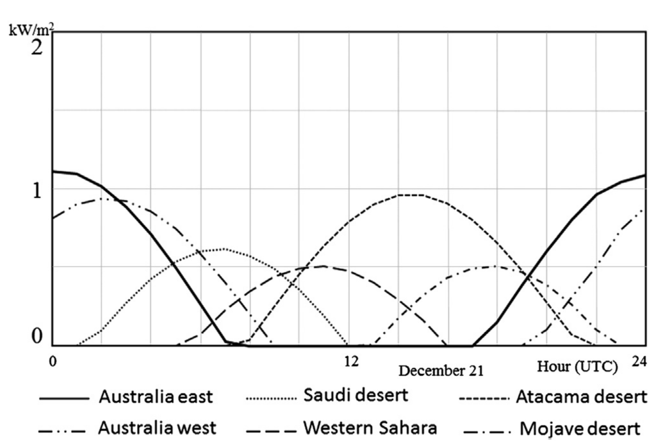


Fig. 2. The distribution of irradiation over a day from M3 for six sites with high insolation.

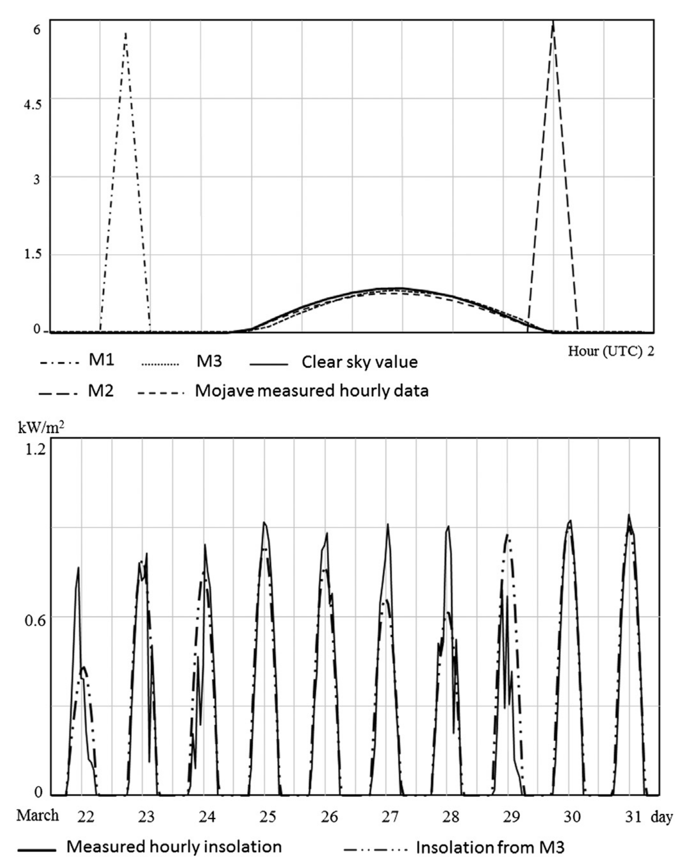


Fig. 3. Top: Insolation as given by M1, M2, and M3 compared with measured hourly data for the Mojave [17], September 21, 2005. Bottom: Comparison of measured hourly data with irradiation according to M3 for 10 day in September 2005.

each day is identical to the daily insolation from Solar Sizer. The reason for this is the different properties of the data sets, which lead to the Solar Sizer data having a lower peak than the measured hourly data. The measured hourly data are for a grid of 1 km × 1 km while Solar Sizer data are for a 1° × 1° grid (about 111 km × 90 km). This averaging over a large area takes out the extremes. In summer irradiation is more even over larger areas and thus M3 is closer to the measured data. In spring and winter the differences between the two data sets are similar to those shown in Fig. 3 (bottom).

Fig. 3 top also illustrates the role of M3 in providing a lower bound for storage. M2 is on the safe side with respect to storage, whereas the pattern of irradiation from M3 could be too elongated on days with below average insolation (as discussed above) possibly underestimating necessary storage.

4. Distributed solar configurations

In this section we review the EUMENA configuration [18–22], the US Solar Grand Plan [24] and the Asian–Australian GRENATEC network [25–28] and investigate how these networks could be

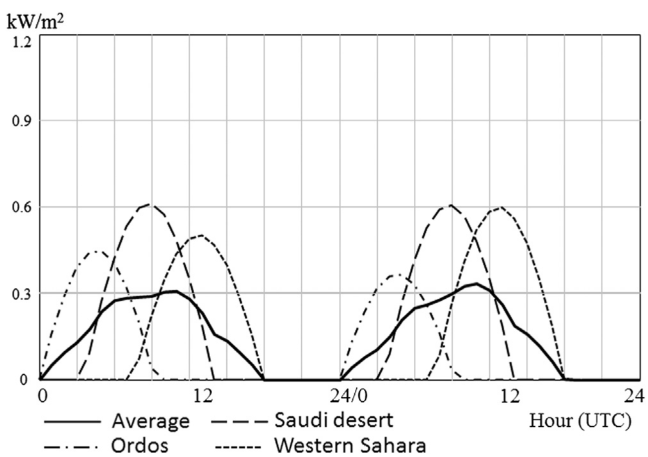


Fig. 4. Availability of sunlight through connecting the EUMENA network with Ordos in the Autonomous Region of Mongolia, China, December 21–22, 2005.

improved. Fig. 4 illustrates the possibility to decrease the time without sun by combining locations in different time zones. Large-scale solar energy networks are also under consideration for other regions, including on a global scale [46–50]. Hence, we will also discuss two global configurations, one with six sites (G6) and one with 15 sites. Table 1 lists all 14 configurations that are discussed in the following.

The cost of electricity from large-scale distributed solar networks has three components: generation, storage, and transmission. The minimum generation capacity and storage required so that a configuration can meet a given load is central for resource (and thus cost) considerations. Our method identifies combination sets of solar sites from an initial set of candidate sites that allow meting a given load with minimal generation capacity and/or storage. The model user can specify whether generation capacity or storage or costs should be minimized. A typical task in planning large solar networks is to determine either the minimal storage with which a load can be met for a given generation capacity, or the minimal generation capacity required for a given amount of storage or the combination of generation capacity and storage that gives the lowest electricity costs. Here we use recent storage cost estimates of 3–5 ¢/kWh [37], and as discussed earlier, LCOE of 5.2 ¢/kWh for an annual insolation of 2300 kWh/m^2, based on projections by First Solar for systems manufacturing costs below $1.20/Wp in 2016 (including 15–20% margin).

We illustrate this optimization for the European, EUMENA and Sahara–Saudi configurations in Section 4.1 where we minimize storage for three different values of generation capacity ('low', 'optimal' and 'high'). For the other configurations discussed here, we also ran simulations for all three values but selected the optimum value for electricity costs as most useful; this is the value presented here.

We find that connecting sites on both hemispheres enables mitigation of the short and low insolation during the northern and southern winters. Our analysis of the Grand Plan, the EUMEMA, the Pan-Asian network, and the G6 network shows that the required storage and generation capacity are lowest when as many time zones as possible on both hemispheres are covered. While the focus of this paper is on the optimization of the costs of storage and generation, we will conclude by briefly discussing current and expected future transmission costs in

Table 1
Configurations for large-scale solar energy generation.

Name	Sites	Geographic region	Location of solar sites
EUMENA7L	7	European Union, Middle East, North Africa	Graz (Austria), Guadix (Spain), Hamburg (Germany), Central Sahara, Egyptian Sahara, Sahara West, Saudi desert
EU10L	10	European Union	Crete (Greece), Graz (Austria), Guadix (Spain), Hamburg (Germany), a site in Italy, Nice (France), Sicily (autonomous island region, Italy), South England, South Germany, South Greece
Sahara–Saudi	4	North Africa, Saudi Arabia	Central Sahara, Egyptian Sahara, westernmost Sahara, Saudi desert
AfricaS8L	8	Southern part of Africa	2 sites in Botswana, 2 sites in Namibia, 3 sites in South Africa, Tanzania
AfricaNS15L	15	Africa south & north	AfricaS8L plus Niger, Saudi desert, 5 sites in the Sahara
NOC	15	Africa, Australia, North and South America	3 sites in the south of Africa, 6 sites throughout Australia, Atacama desert, desert adjacent to Atacama, Mojave desert, Sonoran desert, Sahara/Sudan, Sahara/Yemen
NA3L	3	North America	Chihuahuan desert, Mojave desert, Sonoran desert
NA7L	7	North America	NA3L sites plus Alaska Panhandle, a site in Florida, Koyukuk (Alaska), a site in Texas
PanAm6L	6	North and South America	NA3L sites plus Atacama Desert, site in Argentina adjacent to the Atacama, Bolivia Litoral
China–Mongolia	4	China, Mongolia	East and easternmost Gobi desert (China), Ordos (autonomous area of Inner Mongolia/China), Sukhbaatar (Mongolia).
Australia	7	Australia	Anmatjere, Tanami, central, central-west, eastern, northwest and western Australia
PanAsAu	14	Asia, Australia, Middle East	China–Mongolia and Australia configurations plus Andhra Pradesh (India), Sistan (Iran), site in Pakistan
AsAuSa21L	21	Africa, Asia, Australia, Middle East	PanAsAu and Sahara–Saudi configurations plus a site in Mauritania, Sahara/Sudan, Sahara/Yemen
G6	6	Africa, Australia, Middle East, North and South America	Atacama Desert, eastern and western Australia, Mojave desert, westernmost Sahara, Saudi desert

Section 4.7 and outlining overall electricity cost expectations in Section 4.8.

4.1. A European configuration compared to a EUMENA configuration

The Desertec Foundation has proposed establishing an extensive network of solar and other renewable sites in Europe (EU), the Middle East (ME) and North Africa (NA) (EUMENA) which would supply 80% of the electricity for 30 European countries from renewable energy by 2050 [18–23]. In 2009, the Desertec Foundation and twelve companies from Europe and North Africa established the Desertec Industrial Initiative (DII), a consortium that is furthering the Desertec vision. Planning, bidding and development of solar complexes for several hundred MW each is underway in several MENA countries including Morocco, Algeria, Tunisia, Oman and Jordan [51–53]. The Moroccan Agency for Solar Development (MASEN) recently launched a $9 billion national solar plan that includes three 500 MW installations, one 400 MW and one 100 MW installations [51,52]. The first CSP plant, part of the 500 MW CSP project in Ouarzazate, has received loans near $1.7 billion and substantial investor interest; construction is expected to commence shortly [51]. In Tunisia, DII plans to build a 2 GW CSP plant in collaboration with TuNur, a joint venture of Nur Energie and Tunesian entrepreneurs [54].

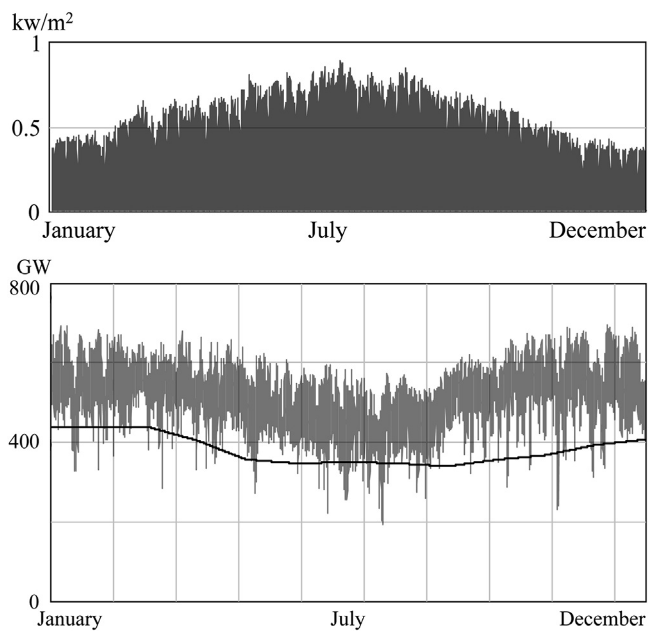


Fig. 5. Top: average insolation in EUMENA7L over one year. Bottom: Electricity generated by the NOC (grey line), a configuration of 15 locations from all over the globe selected and fitted with adequate capacity to meet the EU27 load (black solid line) at all times.

The current plans in the MENA region rely mainly on CSP and wind energy; a design which could now be changed to include PV. We compare a EUMENA-like configuration with seven locations in Europe, the Middle East and North Africa (EUMENA7L, and Fig. 5 top) to a European-only configuration with 10 locations (EU10L) and a Sahara–Saudi-only configuration with four sites (Table 1). The ten sites in EU10L are selected to include as many of the European time zones as possible in one configuration and to represent the different conditions across Europe. Table 2 lists the minimally required storage determined during the three model simulations, 'low', 'optimal' and 'high' generation capacity. The high capacity is only used to explore the degree to which storage can be replaced by generation capacity. Designs with a very high ratio of generation capacity to storage are far too expensive. In order to get lower and upper bounds for the necessary storage, M3 and M2 are both applied; "Ratio M2/M3" gives the relative size of the uncertainty interval. This table shows that the required storage for EUMENA7L and EU10L is at most 1.6, respectively 1.5 times the storage given by M3 for extreme optimization ("High") and at most 1.4, respectively 1.1 times the storage given by M3 for lowest generation costs ("Optimal"). Table 2 also presents the results of the different optimizations for the scaling methods M1, M2 and M3. M1 and M2 give similar results although M2 takes time zones into account while M1 does not. This result is due to the low number of time zones in both configurations.

A major problem for spatially extended networks is investors' perception of risk due to political instability or the inclusion of politically less desirable nations [55]. Consequently, network planners will want to compare several configurations, with and without nations that are potentially viewed as problematic. Hence, we include the Europe-only configuration although it requires considerably more generation capacity (and/or more storage, Table 2). Connecting the sites of the Sahara–Saudi configuration allows electricity generation in winter from 3:00 UTC in the Saudi Desert until 18:00 UTC in the westernmost Sahara. Dealing with the days with the shortest period of sunlight during winter is crucial to minimize storage needs and supplementary energy sources. Electricity generation in this configuration is increased to 15 h, compared to ~11 h for an isolated location in the desert areas. Hence, this configuration needs storage only for about 9 instead of 13 h, and the time for charging storage increases from 11 h to 15 h.

There are clear trade-offs between storage and generation capacity. Storage decreases the required capacity by evening out differences in the insolation of the configuration. High generation capacity reduces the need for storage by allowing the configuration to meet the load also closer to the beginning or end of a day. This relationship is generally non-linear. For example, increasing generation capacity by only ~8.1% from 18.5 GwP to 20 GwP in EU10L decreases storage by ~42.3% for M2 and 44.9% for M3,

Table 2
Methods M1, M2, M3 in comparison for three configurations with a fixed 24/7 load of 1 GW.

Configuration Gen Capacity	EU10L Low	Opt.	High	EUMENA7L Low	Opt.	High	SaharaSaudi Opt.
Gen Cap [GWp]	18.5	20	40	9.8	11.6	19.1	9.8
Storage M1 [GWh]	110.6	65.2	22	61.3	24.9	20.2	24.2
Storage M2 [GWh]	114.5	66.1	22	62.4	23.6	20.1	26.3
Storage M3 [GWh]	107	59	15	56	17	12.8	19.4
Storage max [GWh]	114.5	66.1	22	62.4	24.9	20.2	26.3
Storage min [GWh]	107	59	15	56	17	12.8	19.4
Storage min/max [%]	93	89	68	90	68	63	74
Ratio M2/M3 [%]	107	112	147	111	139	157	136
Capacity factor [%]	16.3	16.3	16.3	20.1	20.1	20.1	24.3
Effect. cap. factor[%]	5.4	5	2.5	10.2	8.6	5.2	10.2

while doubling capacity thereafter to 40 GwP gives a relatively smaller decrease of only 66.7% for M2 and 74.6% for M3. Increasing generation capacity for EUMENA7L by ~1.8% decreases storage by ~62.2% for M2 and 69.6% for M3; whereas a further capacity increase by 7.5% decreases storage only by ~6.3% for M2 and ~24.7% for M3.

Fig. 6 shows the isolines for generation capacity and storage for several configurations, including EU10L and EUMENA7L. Fig. 6 also shows that the optimization of storage as a dependent variable over a range of capacity values from very low to very high follows the shape of a negative exponential. An optimal approximation which minimizes the square of the difference gives the negative exponential f for storage in dependence on generation capacity x.

$$f(x) = 251657 \times e^{-0.000385035\times(x-2779.24)} + 14544.5$$

with a maximum error of 13.7% for $x = 8100$ that decreases to 2.6% for $x = 28{,}800$. The $1/x$ type function

$$g(x) = \frac{5.4098 \times 10^7}{(x-6829)+11218}$$

has a maximum error of 4.7%. Thus, g is a better approximation than f. Fig. 6, bottom, shows these functions for 5 configurations. A surprising result is that this relationship has a $1/x$ type form for all configurations that we analyzed, also if the optimization uses M2 instead of M3.

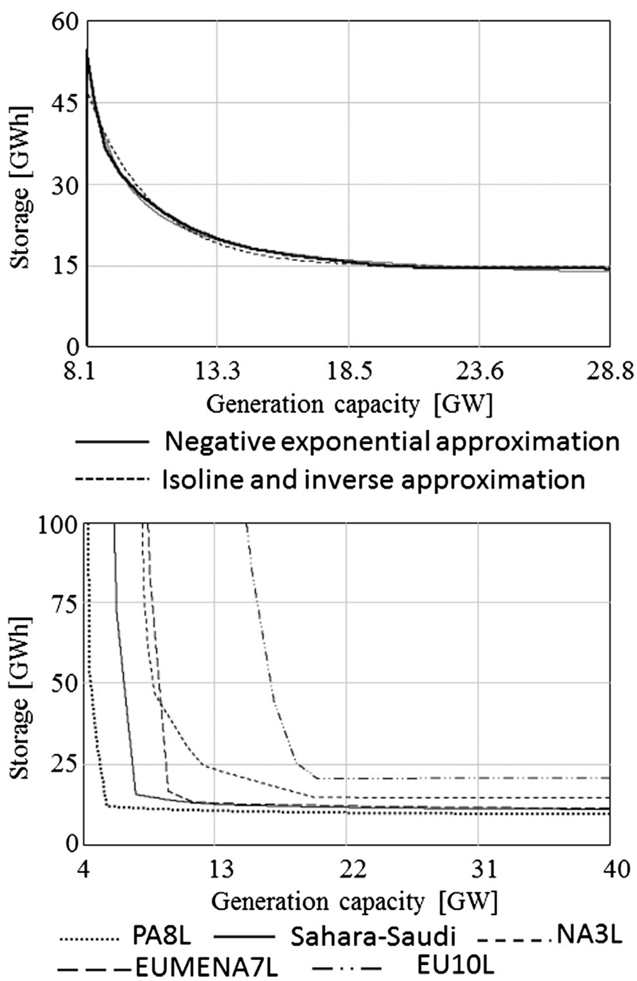


Fig. 6. Isolines for generation capacity and storage to meet a 1 GW load with NA3L (top, given as 5-year average) and PA8L, Sahara–Saudi, NA3L, EUMENA7L and EU10L (bottom, year 1986).

Based on this relationship between generation capacity and storage the minimization of generation capacity through storage is stopped when one additional unit of storage no longer decreases generation capacity noticeably, as in the numeric examples above. Similarly, the minimization of storage through generation capacity is stopped when one additional unit of generation capacity does not noticeably decrease storage.

Table 2 illustrates that generation capacity in the desert is much more productive than in the European locations. Using the optimal values, the EUMENA7L configuration needs a generation capacity of 11.6 GWp to meet a continuous load of 1 GW whereas the EU10L configuration needs 20 GWp. Storage is also lower in the EUMENA7L configuration due to a higher number of time zones and longer days in winter. We find that generation capacity could in fact be even lower (9.8 GWp) if all of it were based in deserts sites, as in the "Sahara–Saudi" configuration. The capacity factors are not as different. This is because during summer the European sites generate excess electricity, which is not visible in the capacity factors. To reflect this, we suggest a new measure, the "effective capacity factor" which takes into account the ratio between electricity generation and demand. It is defined as the constant maximal load that is continuously met divided by the generation capacity. The effective capacity factor measures the degree to which capacity is used, whereas the capacity factor is defined as the percentage of electricity from a panel in a standardized environment divided by the electricity that the panel gives at constant insolation at 1 kW.

4.2. Adaptation to load curves

Table 2 is calculated for a constant load of 1 GW during 1986–2005. Real load curves are nonlinear with three major patterns, a daily pattern, a weekly, and a pattern over the seasons of a year. The optimization can determine locations from the initial set of 67 locations to create a new configuration that meets a given load curve with minimal generation capacity and storage. This allows determining optimal configurations for a national or regional load curve. As an example we consider the load curve for 27 European countries (EU27) for 2011 [56]. The EU27 load curve

Table 3
Feasible pairs of generation capacity ('Gen cap') and storage that would consistently meet the EU27 load curve according to M1, M2 and M3.

Location	EU10L	Eumena7L	AfricaNS15L	AfricaS8L	NOC
Gen cap high [TWp]	35,000	12,600	5,700	8,800	5,226
Storage M1 [TWh]	9,675	8,351	8,405	9,668	2,635
Storage M2 [TWh]	9,660	8,745	8,344	9,632	3,338
Gen cap low [TWp]	7,730	3,892	1,890	2,144	1,941
Storage M1 [TWh]	11,814	10,148	10,268	10,503	3,210
Storage M3 [TWh]	9,600	7,000	7,400	7,600	750
Gen cap optimal [TWp]	8,000	4,200	2,010	2,304	2,986
Storage M3 [TWh]	8,369	6,073	5,745	6,609	33
Capacity factor optimal [%]	16.1	20.3	24.8	23.9	25.6
Effective CF optimal [%]	5.3	10.5	21.5	19	21

has a concave shape, whereas configurations on the Northern Hemisphere such as EUMENA7L give convex patterns of electricity generation (Fig. 5, top). Table 3 lists feasible pairs of generation capacity and storage that would consistently meet this load, based on M2 and M3. Table 3 shows that a purely European solution (EU10L) would be very costly due to its very high demand for generation capacity. The EUMENA-configuration is better but still too expensive. Since the pattern of electricity generated on the Southern Hemisphere is concave like the load curve, we consider a configuration on the Southern Hemisphere, AfricaS8L with eight South African locations (Table 1) and find that it is superior for meeting this load (Table 3). This is a politically interesting result. Even better suited would be an African configuration with sites on both hemispheres ("AfricaNS15L", Table 1), as this additionally allows overcoming the effect of southern winter.

To determine the optimal configuration for this load curve, we start with 67 locations from around the world and minimize the square of the difference between electricity generation and load subject to the condition that the EU27 load curve is always met. We here consider only the annual pattern; however, in addition the optimization could target the daily and weekly load patterns. The contribution of each location is varied by factors between 0 and 5 to find the optimal configuration. The result is a new optimized configuration (NOC) with 15 locations from all over the globe which minimizes the costs of electricity provision (without considering transmission costs) at a generation capacity of 2000 GWp, 657 GWh storage and an effective capacity factor of 21.6%. The curve according to M3 never touches zero so that higher generation capacity should allow meeting the load consistently without storage (at 3000 GWp, effective capacity factor 14.4%, Fig. 5, bottom). The NOC with its wide distribution across the globe is more suitable for meeting the EU27 load curve than EUMENA, EU10L or the two African configurations.

While this optimization demonstrates the advantage of connecting a larger number of widely distributed locations, it highlights problems. The NOC is optimal with regard to storage and generation capacity, but it does not consider criteria such as geopolitical issues or the costs of new transmission networks. The original 67 locations from around the globe are in desert or arid regions or in countries with a strong base in PV (e.g., Germany). The NOC consists of six sites in Australia, two in South America (Atacama and adjacent desert areas), two in North America (Mojave and Sonoran), three in the south of Africa and one each in the southern Sahara in Sudan and Yemen. All European sites were discarded; only one is located in the EUMENA region (Sahara in Sudan). Such a configuration is likely difficult to implement. This optimization shows how much can be gained in economic terms if long-distance transmission is developing well. Widely distributed configurations for other countries or regions may be similarly outstanding in comparison to configurations that are limited to countries and adjacent regions. This would give strong incentives for developing large distributed networks.

Figs. 4 and 5 are not recommendations on electricity generation for Europe, rather, they show the considerable potential of the method presented here for further specific analyses. A method that allows flexible evaluation of a large number of sites on an hourly basis over 20 years, taking into account time zones and seasons for each site is necessary as a basis to analyze economic factors such as transmission costs (which we discuss in Section 4.6), trade balances, and political considerations. Differences in load curves between countries or regions prevent a straightforward comparison of configurations. For example, electricity demand in California has a summer peak while the EU27 load is maximal in winter. To facilitate the comparison of different configurations (and having demonstrated that our method can meet a variable load curve), we proceed using an identical constant load curve for all configurations. The unit of 1 MW which is frequently used in cost calculations is small relative to the EU27 load of around 400 GW (Fig. 7 top) or the global demand of about 2.1 TW. We will use a unit of 1 GW.

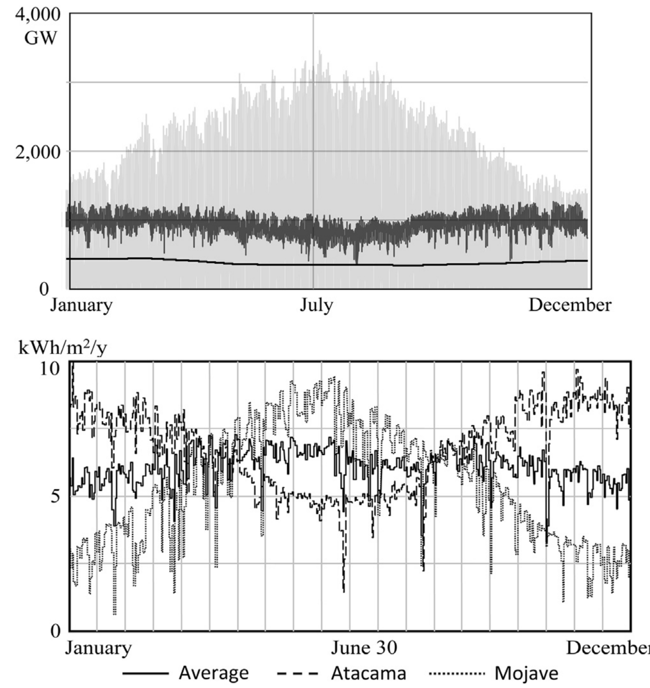


Fig. 7. Top: EU27 load curve and electricity supply through EUMENA7L and the NOC. Bottom: insolation over one year for Atacama and Mojave Deserts and average insolation.

4.3. A US-configuration versus a Pan-American configuration

The Solar Grand Plan proposed by Zweibel et al. 2008 [24, herafter Z08] would supply 69% of the US electricity needs and 35% of the total US energy needs (including transportation) from solar, wind and geothermal by 2050, with a major proportion of solar. Electricity would be transported from desert sites across the US Southwest to major hubs with ultra-high-voltage DC transmission lines (HVDC) at average costs of 2 ¢/kWh. Z08 includes CSP, which is more expensive than PV but can use thermal storage that is cheaper than compressed air energy storage (CAES). Storage of ~250 TW h is needed, more than three times the energy generated daily. The Grand Plan scheme is still affected by intermittency; it relies on auxiliary boiler units heated with natural gas for electricity production when the thermal storage is depleted. The gas required is on the order of 11.7% of the total energy consumed. The generation overcapacity, considerable use of CSP, auxiliary boiler units and fuel are all expensive. Thus, although Z08 can fully cope with intermittency it demonstrates the costs resulting from intermittency and shows also why all large-scale renewable energy plans so far see only a limited role for solar in combination with other forms of renewable energy.

The Grand Plan relies exclusively on sites in the US Southwest, which has too few time zones to enable dramatic reductions in intermittency, and this configuration suffers from the northern winter. To investigate the effect of adding time zones or connecting the two hemispheres, we compare a US configuration consisting of three North American desert sites (the Mojave, Sonoran and Chihuahuan) (NA3L) with an extended US configuration (NA7L, Table 1) and a Pan-American configuration with six sites (PanAm6L, Table 1). We find that the Pan-American extension reduces intermittency to a fraction.

Table 4
Data for two US configurations and a Pan-American configuration.

Configuration	NA3L	NA7L	PanAm6L
Generated [TWh]	40.2	34.0	15.7
Consumption [TWh]	8.7	8.7	8.7
Consume from storage [TWh]	4.4	3.6	3.8
Excess [TWh]	31.4	25.3	7.0
Generation capacity [GW]	20.4	21.0	7.2
Storage capacity [GWh]	16.7	17.3	14.0
Number locations	3	7	6
Capacity factor [%]	22.5	18.5	24.9
Effect cap. factor [%]	4.9	4.8	13.9

Table 5
Data for the China–Mongolia and the Australia configurations.

	China–Mongolia	Australia
Generated [TWh]	27.3	22.9
Consumption [TWh]	8.7	8.7
Consume from storage [TWh]	8.1	4.3
Excess [TWh]	18.5	14.2
Generation capacity [GW]	17.6	10.5
Storage capacity [GWh]	26.4	13.9
Number locations	4	7
Capacity factor [%]	17.7	24.9
Effect cap. factor [%]	5.7	9.5

Table 4 gives key data on these configurations. NA3L generates the highest amount of electricity but only about 20% of this electricity is consumed. In addition to the deserts of NA3L, NA7L includes sites in Florida, Texas and Alaska. In NA7L, about 25% of the generated electricity is consumed at about the same storage and generation capacity. PanAm6LL has only about 1/3 of the generation capacity and slightly lower storage but can meet the same load. This configuration includes the three North American deserts and additionally sites in the Atacama Desert, a site in Argentina adjacent to the Atacama and a site in Bolivia. Fig. 7, bottom panel, illustrates why PanAm6L can handle the load with a much lower generation capacity. Already the combination of one suitable desert from each hemisphere (here the Atacama and the Mojave) results in an average that experiences no winter; the annual average insolation is almost consistently >5 kWh/m^2. Since PanAm6L never experiences winter, it does not need excessive capacity to cope with low winter insolation. This configuration is discussed in much more detail in a companion paper [46].

4.4. A China–Mongolia configuration

China has recently become very active in renewables and in particular in PV. In the past years it has continuously increased its plans for domestic installation of renewable energy and in particular increased planning goals for construction of solar capacity [25,29,57]. China spans almost 4 time zones and has several large desert or arid areas. The China–Mongolia configuration considered here includes three desert sites (a site each in the Gobi Desert and east of Gobi, Ordos in the autonomous region of Inner Mongolia, China), and a site in Sukhbaatar, Mongolia to facilitate linking the Russian and Chinese electricity grids. As there are plans to link the Russian and the European networks, this configuration could also be linked to EUMENA. Linking Ordos to EUMENA7L would increase the number of time zones and extend the shortest period of solar irradiation (in the northern winter) from 15 to almost 18 h (Fig. 4). In summer, this network would have sun for about 23 h.

The sites in the China–Mongolia configuration are at a similar latitude (slightly further north) as the sites in NA3L. Both configurations are situated in the Northern Hemisphere only and thus experience a distinct summer–winter rhythm. This similarity is visible in the similarly low capacity and effective capacity factors (Tables 3 and 4). The China–Mongolia configuration has four time zones compared to the at most 1.5 time zones of the NA3L and NA7L networks; however, this offers only slight improvements to the capacity factor. Noticeable improvements are gained with the 'Australia' configuration (Table 5) that consists of seven sites throughout Australia that cover 2.5 time zones and in particular have only sites at $\sim 22°$S (compared to the Chinese sites at $\sim 45°$N) with a much lower summer–winter difference in insolation and longer days in winter.

4.5. An Asian–Australian configuration

The Asia Pacific Energy Research Centre (APERC) has developed a proposal for linking solar energy generation throughout most of Asia [28]. The Grenatec organization has proposed a large Asian–Australian supranational scheme using solar, hydrogen, and algal fuels [25]. Here, we analyze a configuration with 14 sites (PanAsAu, Table 1), including the 4 sites of the China–Mongolia configuration above and one site each in India, Pakistan and Iran. The balancing of winter on one hemisphere through summer on the other hemisphere is most effective if generation capacities on both hemispheres are similar. Hence, PanAsAu also includes seven sites distributed across Australia.

We find that PanAsAu uses its generation capacity much more effectively than the China–Mongolia configuration and can meet the 1 GW load with 5.6 GWp capacity instead of 17.6 GWp, at a lower storage capacity of 21 GWh instead of 26.4 GWh. At costs of 3–5 ¢/kWh for storage [37] the storage adds about $6.6 \times 4/8.7 = 3.03$ ¢/kWh to the costs of electricity.

4.6. Global configurations

Two global configurations were considered, NOC and G6, both of which could supply a given load without storage. Fig. 7 (top) illustrates that the global configuration NOC can meet the EU27 load at all times during 2011; in fact, according to M3 this would also be possible without storage since the electricity supply never touches zero and can therefore be lifted above the demand curve with sufficiently large generation capacity.

G6 is the minimal combination of the three major schemes discussed above (EUMENA, GRENATEC and the US Solar Grand Plan) with just six sites. Despite the small number of sites, the sum of the insolation in G6 is never zero, enabling it to meet a given load without any storage. At certain times the total insolation is much lower than the average insolation so that a minimal storage would allow meeting a considerably higher load. This is markedly different from the situation of all other configurations (except the NOC) where insolation becomes zero every day. Both the North-American and European configurations additionally need a large capacity in order to fill the storage during the winter months when insolation is low and days are short. This problem is somewhat less pronounced in the Sahara–Saudi and EUMENA7L configurations that cover five time zones compared to the 1–2 time zones covered by the North American and European configurations. A really significant improvement (in terms of the reduction of both the required generation capacity and storage) is only achieved when the two hemispheres are connected.

The storage in G6 configuration never gets close to being empty, with the exception of one day in year 2000 on which two separate Australian locations experienced very low insolation. That day, the East Australian site only received 0.45 kWh/m^2 compared to an average daily insolation of 5.65 kWh/m^2 and the

West Australian site received 1.37 kWh/m^2 compared to an average insolation of 6.15 kWh/m^2. Configurations for solar electricity generation have to be able to deal with such events. According to our evaluations, the most effective approach seems to be to include more locations than just 6 and spread sites across larger areas.

4.7. Transmission costs

We will briefly discuss transmission costs as these decide whether large distributed PV networks can be feasible. The cost of a HVDC-transmission line is the sum of the costs of the transmission cable and the costs of the stations at the beginning and end that convert the AC from the generator to DC and back to AC. Additional costs are caused by electricity losses in the line, estimated at ~2.5–3% per 1000 km of line length and 0.7% per station [58]. PV parks require only one conversion station as they give DC so that the conversion from AC to DC at the beginning is not necessary; an electronically simpler and less expensive switching array suffices to bring the voltage from the PV installation to the required high voltage of the line. To be on the safe side we calculate the full costs of two stations here. HVDC lines with a capacity of 6 GW at 800 kV have been installed in China in 2010 by ABB and Siemens [59]. ABB [59] gives costs of $66.7/1000 km/kW for a line with 6 GW and 800 kV, and station costs of $450 million.

In addition, costs depend on line capacity and utilization. Large solar parks need to be well connected to centers of consumption. Lines connecting both hemispheres have to have sufficient capacity to transmit the missing electricity from the respective other hemisphere during winter. To estimate line utilization, we consider that winter insolation in most desert areas between 30° and 40° latitude is only about 30–40% of summer insolation. Consequently, line utilization during winter will be about 1/3 of summer utilization. At latitudes poleward of 40° this ratio is even less favorable, whereas it is better for the few deserts that are closer to the equator. Here we consider the following generation sites that are close to the equator: a Tanzania site at ~4°S, the Sechura in Peru at ~6°S, and a semi-arid area close to Natal in Brazil at ~6°S.

Transmission line length is typically given by the requirement that it ends at large solar parks in a desert area at ~25°–40° latitude on the respective other hemisphere where it can connect with existing lines to consumption centers. The distance between two solar parks in desert areas at 30°N and 30°S is 6600 km, for sites at 40°N and 40°S it is 8800 km. Actual transmission lines will be longer than the direct distance, for example to avoid oceans that need more expensive submarine cables. The length of a transmission line from Darwin, Australia to Kunming, China that connects locations throughout Indonesia, Singapore, Malaysia and Thailand on the way is ~9200 km; the length of a land line between the Atacama Desert in Chile and San Diego in the US is ~9500 km. We henceforth assume average line lengths of 9500 km for inter-hemispheric connections.

Fig. 8 depicts a prototypical load relative to the insolation generated in a simplified two-site configuration consisting of a Northern Hemispheric desert (Mojave) and a Southern Hemispheric desert (Atacama). The area between the load and the respective surplus and deficit of each hemisphere during its summer and winter gives the amount of electricity exchanged via the inter-hemispheric transmission line. For insolation, we here use the clear sky form over one year for a basic assessment. The typical maximal summer insolation in the Atacama is 1.2 times the typical maximal summer insolation in the Mojave. North America will need ~19% of its total consumption from the Atacama (based on Fig. 8) at costs of 8.2 ¢/kWh (with PV systems costs of $1.20/Wp, as projected by First Solar, and 2400 kWh/m^2/y) including transmission costs of 3.34 ¢/kWh from the Atacama to the Mojave (see below). This consumption of 19% is represented by the area below the cosine curve as long as it is above the load curve at $y=0.75$. The other 81% would be generated in the Mojave at costs of 5.2 ¢/kWh (with PV systems costs of $1.20/Wp at 2300 kWh/m^2/y). Transmission costs within the US of 1–2 ¢ (2 ¢ according to [37] and 1 ¢ with the new 800 kV DC transmission technology based on [59]) yield average costs of $0.19\times 8.20+0.81\times 5.2+1=6.8$ ¢/kWh including generation and transmission.

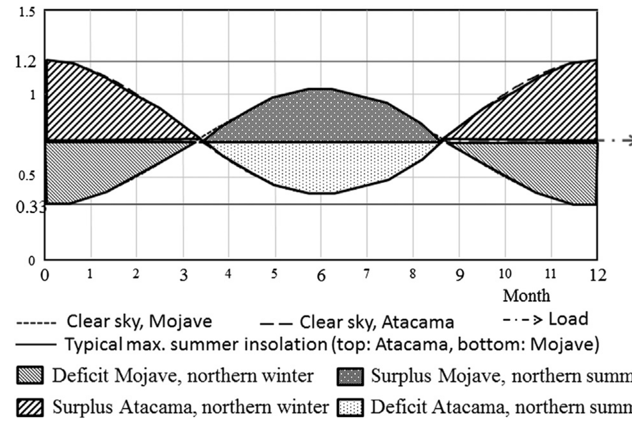


Fig. 8. Scheme for assessing the utilization rate of an inter-hemispheric transmission line.

Table 6
Data for the Pan-Asia-Australia and the Asia–Australia–Sahara configurations.

Item	PanAsAu	AsAuSa21L
Generated [TWh]	10.8	15.0
Consumption [TWh]	8.7	8.7
Consume from storage [TWh]	6.6	2.3
Excess [TWh]	2.1	6.2
Generation capacity [GW]	5.6	7.4
Storage capacity [GWh]	21	8.1
Number locations	14	21
Capacity factor [%]	22.2	23.2
Effect cap. factor [%]	17.9	13.6

Utilization is given by $A_{L,I}/A_{L,U}\approx 55\%$, where $A_{L,I}$ is the area between the load curve and the insolation curve above it (Fig. 8), and $A_{L,U}$ the rectangle between the load curve and the line at 1.2. 55% is a reasonable approximation. The maximum utilization could be $\int_0^{\pi/2}\cos x\,dx/(\pi/2)\approx 0.637$; actual utilization depends on factors such as insolation and load patterns. With the numbers given above, transmission costs over 9500 km for a 6 GW, 800 kV line at 55% utilization are 3.62 ¢/kWh or 3.34 ¢/kWh, respectively, for electricity from the Mojave and Atacama, including losses of ~25% that cause costs of 1.32 ¢/kWh and 1.04 ¢/kWh, respectively. Costs would be about the same for lines between Australia and China. Thus, the costs of receiving electricity from the other hemisphere do not add much to the electricity costs. A realistic cost comparison will also have to take into account that an inter-hemispheric connection will allow significant reductions in required overcapacity, for example, from a factor of almost 5 in a purely solar version of the Grand Plan (the "Generated" electricity in Table 4 divided by the "Consumption") to a factor of 1.24 (from Table 6). This would decrease domestic electricity costs for the ~81% of electricity generated domestically by decreasing generation capacity by this ratio. We note that Z08 limits overcapacity by using burners in all CSP installations.

Transmission costs and losses will continue decreasing as HVDC is at an early stage of its learning curve and most of the transmission capacity has been installed since January 2009 [60]. New transmission technologies under development include pipes made of aluminum instead of copper wires, which is possible for DC but not AC [61], and superconducting cables [62]. DC lines with higher voltages of 1100 kV or 1500 kV are also discussed [63,64]. Future losses have been estimated at $<1\%$ per 1000 km [61].

4.8. Electricity costs given long-distance transmission

As can be seen from Table 6 or more generally from Fig. 6, costs can be minimized through tradeoffs of two types: First, between generation capacity and storage, and second, between longer transmission lines and the use of more generation capacity, storage, or both. For example, increasing generation capacity for PanAsAu by 30% allows decreasing storage by 55%, e.g., from 21 GWh storage with 5.6 GW generation capacity to 11.6 GWh storage with 7.3 GW generation capacity. If transmission costs are not taken into account, a capacity of 5.6 GWp for a load of 1 GW and costs of 1$/Wp gives electricity costs of 6.45 ¢/kWh for a consumption of 8.7 TW h, of which 6.6 TW h are from storage at 3–5 ¢/kWh (Table 6, left column). The storage gives additional costs between 3 ¢/kWh and 5 ¢/kWh multiplied with 6.6/8.7, i.e., between 2.3 ¢/kWh and 3.8 ¢/kWh, with total electricity costs between 8.75 ¢/kWh and 10.25 ¢/kWh. For the configuration AsAuSa21L, electricity costs are 1.5% cheaper.

In a sensitivity analysis corresponding to 1.76 ¢/kWh for an annual average insolation of 2300 kWh/m^2, Zweibel [35] uses a lower limit for PV systems costs of $0.4/Wp. First Solar expects that margins will settle between 10% to 20%, implying an increase from the current zero margins and a decrease from margins $>50\%$ up to 2010. This would give a lower limit of $\sim$2 ¢/kWh for electricity costs.

If the costs of importing PV electricity from South America decreased to $\sim$3 ¢/kWh including costs of transmission, as discussed earlier given considerable line improvements, the US would receive the aforementioned 19% of its electricity at costs of 3 ¢/kWh from the Atacama and the other 81% from domestic sites in the Southwest at costs of 1.8 ¢/kWh with additional 1–2 ¢ of domestic transmission costs. This gives a lower bound for electricity costs of $0.19\times3+0.81\times1.8=2$–3 ¢/kWh, i.e., 3–4 ¢/kWh including domestic transmission.

Using the capacity and effective capacity factor from Table 6, the lowest costs for AsAuSa21L are 1.76 ¢/kWh $\times$ 23.2/13.6 = 3 ¢/kWh for generation, plus $2.3\times4.4/8.7=1.16$ ¢/kWh for electricity from storage, plus 1 ¢/kWh $\times$ 0.19 and 2 ¢/kWh, respectively, for domestic transmission and transmission from the other hemisphere, resulting in total costs of $3+1.16+0.19+2=6.35$ ¢/kWh. This shows that generation is most expensive at 3 ¢/kWh, followed by transmission in the domestic grid at 2 ¢/kWh and storage with 1.16 ¢/kWh. Of course in reality, all three are needed, generation, storage, and transmission.

It remains to be seen to what degree technological development will approach these limits. In any case, PV has become an important player. If large distributed grids become reality, PV could become a major element in a global energy supply system already at its present costs, and even more so with the further decrease in costs projected by manufacturers and learning curves [39].

5. Discussion

The optimality of a large-scale distributed solar configuration depends on the relative costs of storage versus generation capacity, the costs of long-distance lines, and on geopolitical aspects, such as whether a network involving fewer countries or a diverse network with generation sites in a larger number of countries is preferred [66]. Connecting the two hemispheres allows meeting the same load with considerably lower generation capacity and storage, in the cases of the G6 and NOC even without storage. Connecting all time zones over both hemispheres allows configurations that no longer need storage but configurations perform better with some storage. In particular, storage has to be added as an insurance against unknown, unexpected future erratic events. Cost optimal configurations pose political challenges; for example, the minimization of storage and generation capacity for Europe does not include any European solar sites and only two of its 15 locations are in the MENA region.

We find that the effective capacity factor, which we defined earlier to measure the degree to which capacity is used, is in inverse proportional relationship to the costs of generating electricity in a given configuration since it shows how much capacity is needed to meet the load. Its value is usually lower than the common capacity factor. We also find that the ratio between storage and generation capacity is an important indicator of the performance of a given configuration. Minimizing generation capacity increases storage demand, hence it increases relative demand for CSP (which can use inexpensive thermal storage). If the rapid decrease of PV panel manufacturing costs continues, schemes with comparatively high generation capacity and low storage may become the most economical. As the further technological development is only partially predictable, flexible schemes for the assessment and optimization of solar generation capacity, such as the ones presented here (see in particular Fig. 6), are necessary. Storage = 0 appears to be possible for some configurations, but the resulting effective capacity factor is low. The low effective capacity factor for the configuration G6 is due to the low or extremely low insolation on one day out of the 20 years considered.

Our results highlight the critical importance of optimal site selection. The required generation capacity and storage can differ significantly between configurations that supply energy for a similar area. Configurations with inadequate time zone coverage are characterized by either large amounts of excess electricity (and a larger total amount of electricity generated) or a larger required storage. For example, the PanAuSa21L configuration requires only 39% of the storage needed by PanAsAu (Table 6). The proposed Pan-American extension of the North American network reduces the required generation capacity by, respectively, 61% and 54% and storage by 16% and 19% relative to the NA3L and NA7L configurations (Table 4). A detailed analysis of long-term versus short-term storage needs would be of great interest for the G6 configuration.

Electricity from the other hemisphere or from other time zones competes with electricity from storage. Thus, cost optimization needs to consider trade-offs between storage and transmission costs and between different types of storage, in particular thermal storage with costs at ca. 1 ¢/kWh and CAES at ca. 3–4 ¢/kWh. Thermal storage works in connection with CSP plants and is good for up to 24 h. CAES works with electricity from any source and allows storage for months. Given the need for extensive machinery and low efficiency, the costs of CAES will likely not decrease much. However, due to the rapid decrease of costs for PV electricity, the costs of PV with CAES are now below the costs of CSP with thermal storage. Further decrease of costs for PV [1,9,24,65] will shift the balance from slightly more expensive PV generation capacity and ample CAES to higher capacity with less CAES. A mix of CSP and PV can cause problems due to the electricity from CSP being in the form of AC whereas PV gives DC. Consequently, any actual implementation of such networks will need extended research.

Optimization of site selection and the minimization of the required storage and generation capacity are essential to achieve grid parity. Being able to devise and assess large-scale solar electricity networks is a next important step. We have shown that this is only possible at an hourly resolution that accurately reflects differences between time zones. Beyond that, our method enables the significant reduction of oversupply and storage with available data, which will in turn allow considerable cost savings. Together with the expected further decrease of manufacturing costs, in particular for PV, this could help make solar energy competitive with electricity from fossil fuels very rapidly.

Another important result is that the required minimum generation capacity and minimum storage can differ significantly between variations of configurations covering a similar area. This difference is particularly pronounced for expensive long-term storage. Another major result of our analysis is that for most configurations, absolute minimization of storage is only possible with an excessive increase of generation capacity. Similarly, absolute minimization of generation capacity needs excessive storage. Over a very wide range, the relationship between generation capacity and storage can be described with an error of below 5% by simple functions (Fig. 6). The existence of isolines between generation capacity and storage shown in Fig. 6 expands the possibilities for assessing large-scale solar schemes.

These results provide an approach for more detailed assessments of solar energy plans that focus on additional questions, i.e., the positioning of generation sites given geopolitical and environmental concerns, costs and technical feasibility of transmission lines, and fine-tuning of storage and generation capacity by site. We find, for example, that the Sahara–Saudi configuration performs better than the EUMENA-like configuration investigated here. However, one of the advantages of a EUMENA-like configuration is that it spreads generation over a more politically diverse area, resulting in lower vulnerability to energy security threats [39]. Our results provide a method with which such aspects can be evaluated more comprehensively. We discuss such issues in a companion paper for a Pan-American network [46]. As a basis for more detailed assessments such as the one in [46], our method firstly enables the minimization of storage or generation capacity for a given electricity demand. Secondly, it allows optimizing site selection through assessing the effect of including different locations into a large-scale network. These results also provide the basis for possible sensitivity analyses focusing, for example, on the relative importance of different generation sites or different types of storage.

Acknowledgments

The first and third authors were supported by research grants of the Austrian Climate and Energy Fund within the program "New Energy 2020" (project EnergClim) and of the Austrian National Bank (project 14451, DEVELOP). The second author was supported by the Center for Climate and Energy Decision Making created through a cooperative agreement between the National Science Foundation (SES-0949710) and Carnegie Mellon University. The authors thank two anonymous reviewers of this journal for their helpful comments as well as Donald Costello for a review of the scientific computing methods applied here and for numerous helpful suggestions.

References

[1] Bazilian, M, Onyeji, I, Liebreich, M, MacGill, I, Chase, J, Shah, J, et al. Re-Considering the Economics of Photovoltaic Power. Bloomberg New Energy Finance Working Paper 82, May 16, 2012.
[2] Breyer C, Gerlach A, Mueller J, Behacker H, Milner A, Grid-parity analysis for EU and US regions, Proceedings 24th European Photovoltaic Solar Energy Conference 2009, 4492–4500.
[3] Zaman A, Lockman S Solar Industry Growth, Piper Jaffray Investment Research, 2011.
[4] REN21. Renewables 2011 global status report. REN21 Secretariat, Paris, France, 2011.
[5] Breyer C, Gerlach A Global overview on grid-parity event dynamics, 25th European Photovoltaic Solar Energy Conference and Exhibition, 6–10 Sept. 2010, Valencia, Spain.
[6] Zimmermann, A 2012. Extremadura Authority Signs Agreement for Non-subsidized 400 MW PV Project. PVTech. 18 May 2012.
[7] Roca, M Spanish Region Backs $571 Million Solar Plant Without Subsidies. Bloomberg News, May 17, 2012.
[8] Wadia C, Alivisatos AP, Kammen DM. Material availability expands the opportunity for large-scale photovoltaics deployment. Environmental Science and Technology 2009;43:2072–7.
[9] Breyer C, Birkner C, Kersten F, Gerlach A, Goldschmidt JC, Stryi-Hipp G, et al. Research and development investments in PV—a limiting factor for a fast PV diffusion? 25th European Photovoltaic Solar Energy Conference 2010: 5385–408.
[10] Dincer F. The analysis on photovoltaic electricity generation status, potential and policies of the leading countries in solar energy. Renewable & Sustainable Energy Reviews 2011;15:713–20.
[11] Kamat PV, Schatz GC. Nanotechnology for next generation solar cells. Journal of Physical Chemistry 2009;113:1–3.
[12] Unold T, Schock HW. Nonconventional (non-silicon-based) photovoltaic materials. Annual Review Materials Research 2011;41:1–25.
[13] UNEP. 2011. United Nations Environment Programme and Bloomberg New Energy Finance, 2011, Global Trends in Renewable Energy Investment 2011. ISBN: 978-92-807-3183-5.
[14] Lewis NS. Powering the planet. Engineering and Science 2007;2:12–23.
[15] Grossmann WD, Grossmann I, Steininger KW. Indicators to determine winning renewable energy technologies with an application to photovoltaics. Environmental Science and Technology 2011;44:4849–55.
[16] Enerdata, Global energy statistical yearbook 2011, Enerdata 2011. 〈http://yearbook.enerdata.net/〉.
[17] NASA. Radiation Budget Data Products: SSE Surface meteorology and Solar Energy data. NASA Applied Sciences Program 2010.
[18] Desertec. Clean Power from Deserts: the DESERTEC Concept for Energy, Water and Climate Security. Desertec Foundation, Protext Verlag, Bonn, 2009.
[19] Viebahn P, Kronshage S, Trieb F, Lechon Y Final Report on Technical Data, Costs, and Life Cycle Inventories of Solar Thermal Power Plants. German Aerospace Center 2008.
[20] Viebahn P, Lechon Y, Trieb F. The potential role of concentrated solar power (CDP) in Africa and Europe—a dynamic assessment of technology development, cost development and life cycle inventories until 2050. Energy Policy 2011;39:4420–30.
[21] German Aerospace Center, Trans-Mediterranean Interconnection for Concentrating Solar Power. German Aerospace Center 2006.
[22] Desertec Industrial Initiative, 2012. EUMENA 2050: Powered by Renewable Energy. Desertec Industrial Initiative, 16pp.
[23] Trieb F, Schillings C, Pregger T, O'Sullivan M. Solar electricity imports from the Middle East and North Africa to Europe. Energy Policy 2012;42: 341–53.
[24] Zweibel K, James M, Fthenakis V. Solar grand plan. Scientific American 2008;298:64–73.
[25] Grenatec, 2012. Pan-Asian Energy Infrastructure: Outlook 2012. Grenatec Pty Ltd. 2012.
[26] Taggart S, James G, Dong ZY, Russel C. The future of renewables linked by a transnational Asian grid. Proceedings of the IEEE 2012;100(2):348–59.
[27] Taggart S. Unlocking Asia's renewable energy potential. Renewable Energy Focus 2010;11:58–61.
[28] Asia Pacific Energy Research Centre. 2004. Electric Power Grid Interconnections in the APEC Region. Tokyo, Japan, ISBN 4-931482-28-7.
[29] Wang Z. Prospectives for China's solar thermal power technology development. Energy 2010;35:4417–20.
[30] Pew Charitable Trusts. 2011. Who's winning the clean energy race. Pew Charitable Trusts.
[31] Zweibel, K 2005. The Terawatt Challenge for Thin-Film PV. National Renewable Energy Laboratory 2005, Technical Report NREL/TP-520-38350.
[32] Photovoltaic Production, 2012. Squeezed Margins: Crystalline PV Module Profits Fall to Single Digits. Photovoltaic Production, July 17, 2012. Online: 〈http://www.photovoltaic-production.com/3746/squeezed-margins〉, accessed 2012/07.
[33] Wilkinson, S 2012. PV Module Costs and Prices: What is Really Happening Now? PVTech, 01 February 2012.
[34] Ahearn, M, Widmar, M, Brady, D, 2011. First Solar 2012 Guidance. 〈www.firstsolar.com〉, Section Investor Relations, accessed Dec. 14, 2011.
[35] Zweibel, K, 2005. Thin Films and the System-Driven Approach. NREL/CP-520-36968.
[36] Solarbuzz, 2012. Top-tier photovoltaic polysilicon and wafer producers to be profitable in 2013. Solarbuzz July 2, 2012. Online: 〈http://www.solarbuzz.com/news/recent-findings/top-tier-photovoltaic-polysilicon-and-wafer-producers-be-profitable-2013〉, accessed July 31, 2012.

[37] Fthenakis V, Mason JE, Zweibel K. The technical, geographical, and economic feasibility for solar energy to supply the energy needs of the US. Energy Policy 2009;37:387–99.
[38] US Energy Information Administration. 2012. State Electricity Profiles. Online: 〈http://www.eia.gov/electricity/state/〉, accessed June 2012.
[39] Grossmann, WD, Steininger, KW, Schmidt, C, Grossmann, I Investment and Employment from Large-Scale Photovoltaics up to 2050. Empirica Special Issue 'Climate and Global Change, Selected Papers from the 2011 Annual Meeting of the Austrian Economic Association' 39: 165–189.
[40] Baños R, Manzano-Agugliaro F, Montoya FG, Gil C, Alcayde A, Gomez J, et al. Optimization methods applied to renewable and sustainable energy: a review. Renewable and Sustainable Energy Reviews 2011;15:1753–66.
[41] Zahedi A. Maximizing solar PV energy penetration using energy storage technology. Renewable and Sustainable Energy Reviews 2011;15:866–70.
[42] Czekalski D, Chochowski A, Obstawski P. Parameterization of daily solar irradiance variability. Renewable and Sustainable Energy Reviews 2012;16: 2461–7.
[43] Milone EF, Wilson W. Solar System Astrophysics: Background Science and the Inner Solar System. Springer; 2008.
[44] Spencer JW. Fourier Series Representation of the Position of the Sun. Search 1971;2(5).
[45] National Renewable Energy Laboratory. National Solar Radiation Data Base (NSRDB): USAF #722953—MOJAVE, CA. National Renewable Energy Laboratory, Golden, CO, 2007. Online: 〈http://rredc.nrel.gov/solar/old_data/nsrdb/〉, accessed November 2010.
[46] Grossmann WD, Grossmann I, Steininger KW Solar electricity generation across large geographic areas, Part II: A Pan-American energy system based on solar. Renewable and Sustainable Energy Reviews (submitted).
[47] Meisen P, Pochert O A Study of Very Large Solar Desert Systems with the Requirements and Benefits to Those Nations Having High Solar Irradiation Potential. Global Energy Network Institute (GENI), San Diego, California.
[48] Jacobson MZ, Delucchi MA. Providing all global energy with wind, water and solar power, Part I: Technologies, energy resources, quantities and areas of infrastructure and materials. Energy Policy 2011;39:1154–69.
[49] Delucchi MA, Jacobson MZ. Providing all global energy with wind, water and solar power, Part II: Reliability, system and transmission costs, and policies. Energy Policy 2011;39:1170–90.
[50] Breyer C, Knies G Global energy supply potential of concentrating solar power. SolarPACES Conference, 15–18 Sept. 2009.
[51] Desertec Industrial Initiative, No Date. Country Focus Morocco. Desertec Industrial Initiative, 2pp.
[52] Lorca, A, Arce, R.de, Abbassi, IE, Bouhadi, AE, Escribano, G, Khellaf, A, et al., 2012. Renewable Energies and Sustainable Development in the Mediterranean: Morocco and the Mediterranean Solar Plan. FEMISE Research Program FEM34-02, 143pp.
[53] Stambouli AB, Khiat Z, Flazi S, Kitamura Y. A review on the renewable energy development in Algeria: current perspective, energy scenario and sustainability issues. Renewable and Sustainable Energy Reviews 2012;16:4445–60.
[54] Stenzel, T, 2012. TuNur: Solar Energy Export from Tunisia to Europe. 2nd EMIS Forum, Tunis, 25–26th June 2012.
[55] Patt A, Komendantova N, Battaglini A, Lilliestam J. Regional integration to support full renewable power deployment for Europe by 2050. Environmental Politics 2011;20(5):727–42 September 2011.
[56] ENTSOE (European Network of Transmission System Operators for Electricity), 2012. Consumption data. Online: 〈www.entsoe.eu〉.
[57] Semiconductor Today. 2011. First Solar and China Guangdong Nuclear to co-develop Ordos project. 7 January 2011.
[58] Bahrman, M 2006. HVDC Transmission. IEEE PSCE, Atlanta, November 1, 2006.
[59] ABB. 2010. Ultra High Voltage DC Systems. ABB Power Technologies AB Grid Systems- HVDC. Ludvika, Sweden, 〈www.abb.com/hvdc〉.
[60] Joint Research Center, 2010. Towards the Super Grid for More Renewable Energy. Renewable Energy Snapshots (July 2010).
[61] Faulkner, R, Todd, R, 2010. PCT Patent Application PCT/US2010/048719 Underground Modular High-Voltage Direct Current Electric Power Transmission System.
[62] Hassenzahl WV, Eckroad SEC, Grant PM, Gregory B, Nilsson S. A high-power superconducting DC cable. IEEE Transactions on Applied Superconductivity 2009;19(3).
[63] Liu, Z, Gao, L, Wang, Z, Yu, J, Zhang, J, Lu, L, 2012. R&D progress on $\pm$1100 kv UHVDC technology. 44th CIGRE Session, Aug. 26–31, 2012, Paris, France.
[64] Huang H, Kumar D, Ramaswami V, Retzmann D Concept Paper on Development of UHVAC System in India. Siemens AG, Germany, 2010.
[65] Bensebaa F. Solar Based Large Scale Power Plants: What is the Best Option? Progress in Photovoltaics. Research and Applications 2010 http://dx.doi.org/10.1002/pip.998.
[66] Marktanner M, Salman L. Economic and geopolitical dimensions of renewable vs. nuclear energy in North Africa. Energy Policy 2011;39:4479–89.